

Dynamics and Quasicontinuum Analogues of a Lattice with Simple Microstructures

M. Charlotte
Université de Toulouse, ISAE
Institut Clément ADER, France

Abstract

The non-trivial behaviour of a simple, linear elastic, monoatomic chain is analysed and then homogenized/continualized/continuumized by taking into account its dispersive properties. These are hardly known and provide nontrivial long-range causal features in the case of an unbounded domain. It is shown that this granular behaviour can be interpreted within continuum models by the presence of pseudo-post-newtonian inertial forces. The last are usually ignored from the multi-scale numerical coupling methods that are based on a hypothetical Hamiltonian decomposition of the energy.

Keywords: lattice dynamics, continualization, enhanced continuum model, inertial forces, wave dispersion, percussion loads.

1 Introduction

With the miniaturization of engineering and the increasing precision of measuring instruments, the use of multiscale numerical methods that couple (possibly generalized) continuum models with atomistic ones increasingly became necessary to account for and justify the behavior of micro-structures [1]. The dynamic behavior of the simplest discrete elastic structures is actually already very complex in the linear regime because of the presence of multiple internal scales of times and lengths [2, 3, 4, 5, 6]. For discrete structures that can be described as atomic lattices, this complexity is embedded into phonon dispersion relations that are highly non-trivial, but relatively well-known in some cases although. To describe the behavior of such structures on a macroscopic scale, many numerical approaches (e.g. finite element method (FEM), generalized FEM, eXtended FEM, discrete Galerkin method, smoothed-particle hydrodynamics, quasicontinuum method, etc.) naively rely on the classical continuum (CC) theory that is non-dispersive as a consequence of neglecting the *material intrinsic lengths*

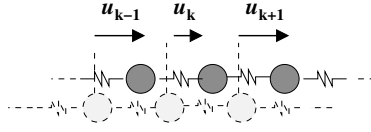


Figure 1: *The infinite monoatomic chain.*

and times of reaction. The CC theory gives however only a very limited description of the singular behavior of the discrete microscopic structure, since it is supposed to handle only waves of deformation with both very long wavelengths and very low frequencies, as illustrated hereafter. Many important physical effects such as acoustic gaps, dispersion, damping and localization of structural vibration modes [2, 7], and micro-instabilities [8] are therefore missed. As a matter of fact, all these phenomena are not relevant to the structures of macroscopic size, but actually become dominant at the scale of the considered microstructures.

In order to provide a theoretical illustration this work considers a very common analytical model that usually serves of comparison for the developments of generalized continuum models [3, 9, 10, 11, 12, 13, 14] and numerical coupling methods involving multi-scales and/or multi-physical models [15, 16, 17, 18, 19, 20, 21]. This concerns the non-trivial dynamic behavior of a simple monoatomic chain with linearly elastic interactions between nearest neighbour atoms (cf. Fig 1) and its equivalent (quasi-)continuum modeling. Within the considered granular model the atoms are only allowed to move colinearly (either longitudinally or transversally to the chain) with $\mathbf{u}(t) = \{u_k(t)\}_{k \in \mathbb{Z}}$ denoting the atomic displacements from the homogeneous lattice equilibrium position. Historically, that discrete model has notably inspired the Isaac Newton's works on the calculus of the sound speed in the air, as well as Jean (I) and Daniel Bernoulli's works on the analysis of vibrating systems [2, 7]. This academic model has some dispersive properties/dynamics that are poorly known in the literature; in particular, they are incompatible with the causal restrictions that [9, 10] require to *consistently* generalize the elastic continuum mechanics.

The works in [4]-[6] have proposed a new analysis that is based on our contemporary mathematical analysis knowledges (Fourier and Laplace transforms, complex analysis, and tempered distributions) to characterize the quasi-continuum dynamics of such a granular material with its main ingredients: impulse response, spatial and temporal properties, and spectrum. This work proposes a brief summary of these analyses for an unbounded domain. Mainly, it is shown in particular that two formulations of continuous accurate interpolations are possible; the first one corresponds to the Eringen and Kunin models of quasi-continua (EKQ, which are based on the Whittaker-Shannon-Kotel'nikovs (WSK) interpolation functions but are then valid or accurate only for unbounded domains); the other is based on a weak spectral multi-polar approximation (WMPA, which is comparable to a multi-point Padé's approximation). In terms of numerical coupling [20], the first continualization method belongs to those methodologies assuming the existence of energy potentials, and the second one to the generalized force-based or virtual power category. Both continualizations involve length

or/and time scales that are non-arbitrary but are related to the dispersive and attenuation structural properties of the atomic interactions [2]. It is shown that the WMPA provides an interpolation of the displacement field of the generic discrete model that superimposes two kinematic contributions: one of them corresponds to the solution predicted by the EKQ and converges for increasing time to the classical theory of elastic continuum; the second contribution has for effects to restrict the oscillations of the first field and vanishes for increasing time. It is shown that a second improved approximation of the classical theory of elasticity can be artificially taking into account the simultaneity of the atomic response, associated with the violation of Einstein's causality. It is shown that this non-trivial behavior can be interpreted in a continuous model by the presence of inertial and pseudo-dissipative post-Newtonian forces that are ignored by most multi-scale numerical coupling methods.

For illustration and clarity, this communication considers only the free motion of an unbounded chain; no external load is applied and no internal collision is allowed for time. More general kinematic and loading conditions were considered in [6] while the case of bounded domains will be presented elsewhere.

2 Free motion of the infinite system

2.1 Equations of motion

Let $a > 0$ be the reference scale length or lattice parameter of the considered chain model. The mass of each atom ρa is then defined with a lineic mass density $\rho > 0$. Moreover, within the harmonic approximation, the atom interactions are ensured by weightless springs with elastic stiffness αa defined with an elastic modulus $\alpha > 0$. Usually, those constants allow to coarsely assess the time $\omega_*^{-1} \stackrel{\text{def}}{=} \frac{a}{2} \sqrt{\frac{\rho}{\alpha}} = \frac{a}{2c}$ and the propagating wave speed limit $c \stackrel{\text{def}}{=} \sqrt{\frac{\alpha}{\rho}}$ that are specific from the macroscopic viewpoint of the classical "homogeneization" based on the long wavelength deformations.

The generalized function theory of causal evolutions [28, 29] provides a natural adequate framework to describe the motion of the chain and to highlight some links with the weak and strong formulations used in numerical methods. Within this framework, the free dynamic motion of the chain that is governed by the equation

$$\rho D_t^2 u_k = \frac{\alpha}{a^2} [u_{k+1} + u_{k-1} - 2u_k], \text{ for } (k, t) \in \mathbb{Z} \times \omega_*^{-1} \mathbb{R}^+ \quad (1a)$$

with the nonzero initial conditions of displacements and velocities

$$\mathbf{u}(0) = \{u_k(0)\}_{k \in \mathbb{Z}} \text{ and } D_t \mathbf{u}(0^-) = \{\dot{u}_k(0^-)\}_{k \in \mathbb{Z}} \quad (1b)$$

becomes (see [6] for further details)

$$\rho D_t^2 [H u_k] = \frac{\alpha}{a^2} H [u_{k+1} + u_{k-1} - 2u_k] + \rho \mathfrak{D}_t^2 u_k, \text{ for } (k, t) \in \mathbb{Z} \times \omega_*^{-1} \mathbb{R} \quad (2a)$$

with the nonzero initial kinematic conditions reinterpreted in terms of localized inertial forces of percussion

$$\rho a \mathcal{D}_t^2 \mathbf{u}(t) = \rho a \left[D_t \mathbf{u}(0^-) \delta_+(t) + \mathbf{u}(0^-) D_t \delta_+(t) \right]. \quad (2b)$$

Those last ones are required to move the chain instantaneously from an “artificial rest state” to the configuration with the given initial displacement and velocity. Those expressions appropriately involve the generalized partial derivative operator D_t with respect to the time variable t of the Heaviside’s step function $H(t) \stackrel{\text{def}}{=} \begin{cases} 0 & , \text{ if } t < 0 \\ 1 & , \text{ if } t \geq 0 \end{cases}$

and the “causal” Dirac’s delta function $\delta_+ \stackrel{\text{def}}{=} D_t H$. The foregoing mechanical model is fully characterized by its elastic and kinetic energies, whose the expressions are well-known. But for the purpose of making comparison the ensuing expression of external work can be also used [6]

$$\begin{aligned} \mathcal{P}_r(\rho \mathcal{D}_t^2 \mathbf{u}(t), \mathbf{u}, t) &\stackrel{\text{def}}{=} a \sum_{k \in \mathbb{Z}} \int_{-\infty}^t \rho \mathcal{D}_t^2 u_k(\hat{t}) D_t u_k(\hat{t}) d\hat{t} \\ &= H(t) \rho a \sum_{k \in \mathbb{Z}} \left[D_t u_k(0^-) D_t u_k(0^+) - u_k(0^-) D_t^2 u_k(0^+) \right]. \quad (3) \end{aligned}$$

2.2 Spectral Characterization

The two problems (1) and (2) can be solved by combining the Laplace’s transform (**LT**) on the time variables $t \in \omega_*^{-1} \mathbb{R}^+$ and the discrete Fourier’s transform (**DFT**) on spatial variables $ka \in a\mathbb{Z}$. The first transform is taken like

$$\tilde{y}(t) \rightarrow \tilde{y}(\omega) = \int_0^\infty \tilde{y}(t) e^{-i\omega t} dt, \quad \Im m(\omega) < -\check{\omega}_b \leq 0, \quad (4)$$

where a sufficiently large constant value $\check{\omega}_b$ is taken to ensure the existence of the integral as a function over a semi-plane of the complex plane $\omega_* \mathbb{C}$. Here $\Re e(\cdot)$ and $\Im m(\cdot)$ denote respectively the real and imaginary parts of the complex number in argument; i is the principal square-root determination of the imaginary number related to $i^2 = -1$. The second transform is defined like

$$\mathbf{y} = \{y_k\}_{k \in \mathbb{Z}} \rightarrow y(\lambda) = a \sum_{k \in \mathbb{Z}} y_k e^{-ik\lambda a}, \quad \forall \lambda \in \mathbb{K} \stackrel{\text{def}}{=} [-\pi/a, \pi/a], \quad (5)$$

but, albeit being restricted to the first Brillouin’s zone \mathbb{K} , is assumed to have an analytical continuation almost everywhere along $a^{-1} \mathbb{R}$ and onto a larger subdomain of the spectral reciprocal complex plane $a^{-1} \mathbb{C}$. The foregoing transforms (4) and (5) have respectively for inverse formulae

$$\tilde{y}(\omega) \rightarrow \tilde{y}(t) = \frac{1}{2\pi} \int_{-i\omega_b - \infty}^{-i\omega_b + \infty} \tilde{y}(\omega) e^{i\omega t} d\omega, \quad \forall \omega_b > \check{\omega}_b \geq 0, \quad \text{for } t \in \omega_*^{-1} \mathbb{R}, \quad (6a)$$

$$y(\lambda) \rightarrow y_k = \frac{1}{2\pi} \int_{-\pi/a}^{\pi/a} y(\lambda) e^{ik\lambda a} d\lambda, \quad \text{for } k \in \mathbb{Z}; \quad (6b)$$

those integrals being defined in the sense of Cauchy's principal values.

The combined application of the transforms (4) and (5) on Eq.(2a) provides then

$$\Phi(\lambda, \omega) u(\lambda, \omega) = \rho \mathfrak{D}_t^2 u(\lambda, \omega) , \text{ with } \mathfrak{D}_t^2 u(\lambda, \omega) = i\omega u(\lambda, 0) + \dot{u}(\lambda, 0^-) \quad (7a)$$

while the holomorphic function of two complex variables $(\lambda, \omega) \in a^{-1}\mathbb{C} \times \omega_*\mathbb{C}$

$$\Phi(\lambda, \omega) \stackrel{\text{def}}{=} \frac{4\alpha}{a^2} \sin^2(\lambda a/2) - \rho\omega^2 \quad (7b)$$

fully characterizes the elasto-dynamical mechanical properties of the discrete material system. The following equivalence (with $q \in \mathbb{Z}$) and characteristic equation

$$\Phi(\lambda, \omega) \equiv \frac{4\alpha}{a^2} [\sin^2(\lambda a/2) - \sin^2(\lambda_q a/2)] = 0 , \text{ for } (\lambda, \omega) \in a^{-1}\mathbb{C} \times \omega_*\mathbb{C} \setminus \mathcal{C} \quad (8)$$

defines for $\omega \in \omega_*\mathbb{R}$ the curves of dispersion [2, 6] that describe the roots $\{\lambda_q(\omega)\}_{q \in \mathbb{Z}}$, those roots being well-defined for $\omega \notin \mathcal{C} \stackrel{\text{def}}{=}]-\infty, -\omega_*] \cup [\omega_*, \infty[$ like

$$\lambda_{2q}(\omega) = \lambda_o(\omega) + 2q\pi/a , \quad \lambda_{2q+1}(\omega) = -\lambda_{2q}(\omega) \quad (9a)$$

$$\lambda_o(\omega) \stackrel{\text{def}}{=} -\frac{2}{a} \arcsin(\omega/\omega_*) , \text{ with } |\Re(\lambda_o)|a \leq \pi . \quad (9b)$$

For each $q \in \mathbb{Z}$, the doublet $(\lambda_{2q}, \lambda_{1-2q})$ lays inside the strip

$$\mathbb{B}_q \stackrel{\text{def}}{=} \{ \lambda = \lambda_r + i\lambda_i \in a^{-1}\mathbb{C} ; |\lambda_r a - 2q\pi| \leq \pi , (\lambda_i a, \lambda_r a) \in \mathbb{R}^2 \} ,$$

the first strip \mathbb{B}_0 containing in particular the fundamental Brillouin's interval \mathbb{K} .

2.3 Spatio-temporal evolution

The solution of the Eq. (1) can be expressed indifferently like (see [6] and also [7, 30, 3]),

$$u_k(t) = \sum_{p \in \mathbb{Z}} \left[u_p(0) D_t \widehat{G}(ka - pa, t) + \dot{u}_p(0^-) \widehat{G}(ka - pa, t) \right] ; \quad (10a)$$

$$\equiv \sum_{p \in \mathbb{Z}} \left[u_p(0) D_t \widehat{G}_K(ka - pa, t) + \dot{u}_p(0^-) \widehat{G}_K(ka - pa, t) \right] , \quad (10b)$$

which for $(k, t) \in \omega_*^{-1}\mathbb{R} \times \mathbb{R}^+$ are equivalent to the solution of Eq. (2)

$$\mathbb{H}(t) u_k(t) \equiv \sum_{p \in \mathbb{Z}} \int_0^t G(ka - pa, t - \hat{t}) \mathfrak{D}_t^2 u_p(\hat{t}) d\hat{t} ; \quad (11a)$$

$$\equiv \sum_{p \in \mathbb{Z}} \int_0^t G_K(ka - pa, t - \hat{t}) \mathfrak{D}_t^2 u_p(\hat{t}) d\hat{t} . \quad (11b)$$

In Eq.(10) the functions

$$\widehat{G}(s, t) = \text{sign}(t) G(s, |t|) \text{ and } \widehat{G}_K(s, t) = \text{sign}(t) G_K(s, |t|) \quad (12)$$

represent respectively the acausal extensions to $(s, t) \in a\mathbb{R} \times \omega_*^{-1}\mathbb{R}$ of the causal Green function interpolation

$$G(s, t) \stackrel{\text{def}}{=} \frac{2\text{H}(t)}{\pi\omega_*} \left\{ \int_0^{\omega_*} \frac{\sin(\omega_r t) \cos\left(\frac{s}{\ell_-}\right)}{\omega_r \sqrt{1 - \frac{\omega_r^2}{\omega_*^2}}} d\omega_r - \sin\left(\frac{|s|\pi}{a}\right) \int_{\omega_*}^{+\infty} e^{-\frac{|s|}{\ell_+}} \frac{\sin(\omega_r t)}{\omega_r \sqrt{\frac{\omega_r^2}{\omega_*^2} - 1}} d\omega_r \right\} \quad (13)$$

and of the causal pseudo-Green function interpolation

$$G_K(s, t) \stackrel{\text{def}}{=} \text{H}(t) \int_0^{\pi/a} \frac{a \sin(\omega_* t \sin(\lambda a/2)) \cos(\lambda s)}{\omega_* \sin(\lambda a/2) \pi} d\lambda. \quad (14)$$

Those functions are defined with two lengths $\ell_{\pm}(\omega)$ that are like

$$\frac{a}{\ell_-(\omega)} \stackrel{\text{def}}{=} \cos^{-1} \left(1 - 2 \frac{\omega^2}{\omega_*^2} \right) \in [0, \pi] \quad , \text{ for } \omega \in [-\omega_*, \omega_*]; \quad (15)$$

$$\frac{a}{\ell_+(\omega)} \stackrel{\text{def}}{=} \ln \left[\frac{2\omega^2}{\omega_*^2} - 1 + \frac{2|\omega|}{\omega_*} \sqrt{\frac{\omega^2}{\omega_*^2} - 1} \right] \geq 0 \quad , \text{ for } \omega \in \omega_*\mathbb{R} \setminus [-\omega_*, \omega_*], \quad (16)$$

which characterize the intrinsic properties of *dispersion* and *attenuation* of the considered *periodic granular media* [2]. Besides $G(s, t)$ and $G_K(s, t)$ are also linked as

$$G(ka, t) \equiv G_K(ka, t) \equiv \text{H}(t) \int_0^t J_{2k}(\omega_* \hat{t}) d\hat{t} \text{ and } G_K(s, t) \equiv \sum_{q \in \mathbb{Z}} \text{sinc}(s/a - q) G(qa, t),$$

with the *Bessel's functions of first type with entire order* [22]

$$J_n(\tau) \stackrel{\text{def}}{=} \frac{a}{\pi} \int_0^{\pi/a} \cos(\tau \sin(\lambda_r a) - \lambda_r n a) d\lambda_r \equiv (-1)^n J_{-n}(\tau), \text{ for } (n, \tau) \in \mathbb{N} \times \mathbb{R}$$

and the *sinus cardinal* function [23, 24]

$$\text{sinc}(\eta) \stackrel{\text{def}}{=} \frac{\sin(\pi\eta)}{\pi\eta}, \text{ for } \eta \in \mathbb{R}.$$

Figs. 2, 3 and 4 illustrate the interpolations of the free motions of the atoms released with $u_k(0^\pm) = \bar{u}\delta_{k,0}$ and $\dot{u}_k(0^\pm) = \bar{v}\delta_{k,0}$, based on (13); here \bar{u} and \bar{v} are given constants, and $\delta_{k,p}$ denotes the Kronecker's symbol. For the CC theory, a non-trivial feature of such a *boundary-less granular structure with weightless interaction springs*, and that is embedded into the Bessel function properties, is that localized initial (kinematic or dynamic) disturbances are redistributed through the infinite structure with infinite velocity (see [30]) by transiently evanescent phonic waves. Instead, the

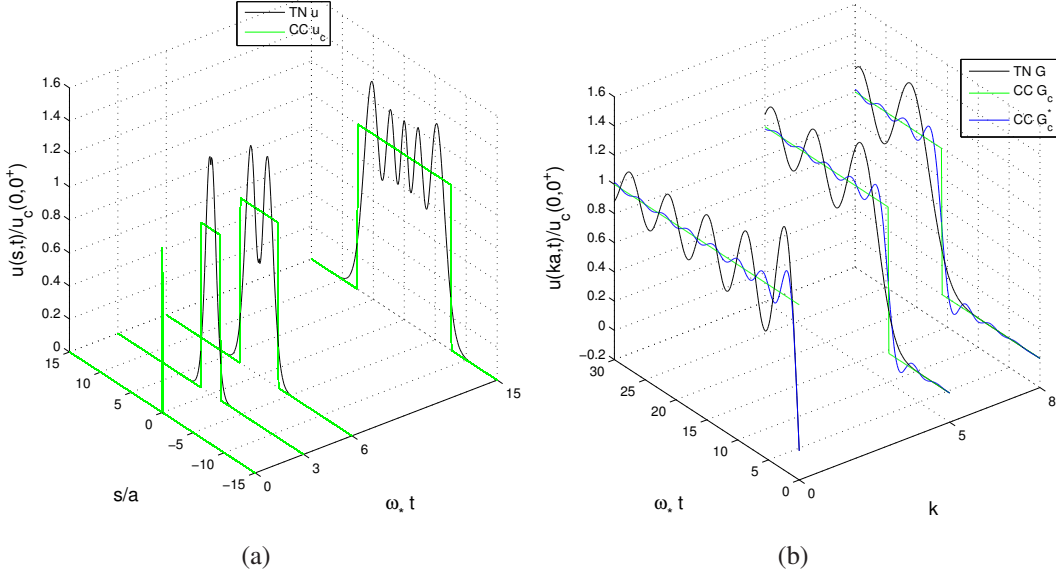


Figure 2: *TN and CC displacement fields resulting from various continuum representations of the discrete initial percussion load $\rho a \bar{v} \delta_{k,0} \delta_+(t)$ $\}_{k \in \mathbb{Z}}$:*
 (a) *the interpolating displacement field $u(s,t) = G(s,t) \bar{v}$ (in black) of the section 2.4.3 generated by the initial inertial load density $\rho \mathcal{D}_t^2 u(s,t) = \rho \mathcal{D}_t^2 u_0(t) \delta(s/a)$ and the CC solution $u_c(s,t) = G_c(s,t) \bar{v}$ (in green) generated by $\rho \mathcal{D}_t^2 u_c(s,t) \equiv \rho \mathcal{D}_t^2 u(s,t)$, with so $\kappa_{c,1}(\eta) = \delta(\eta)$;*
 (b) *comparison of those displacement fields with the smooth one $u_c(ka,t) = G_{c,1}^*(ka,t) \bar{v}$ (in blue) generated by $\rho \mathcal{D}_t^2 u_c(s,t) = \rho \mathcal{D}_t^2 u_0(t) \text{sinc}(s/a)$, with so $\kappa_{c,1}(\eta) = \text{sinc}(\eta)$, for $(k,t) \in \mathbb{Z} \times \omega_*^{-1} \mathbb{R}^+$.*

CC theory assumes that the corresponding energy transferred by those fast phonons are macroscopically negligible and interprets the supersonic transferred energy as infinite and localized along Stokes' rays [6]. This “supersonic” phenomenon violates the Einstein's interpretation of the causality criterion, which may be thought necessary to *consistently* generalize the elastic continuum mechanics [10, 9]. Currently, this latter is expressed with the hyperbolic equations of the CC theory, which in the case of a bar or vibrating string amounts to the D'Alembert's elastodynamic wave one

$$\rho D_t^2 u_c = \alpha D_s^2 u_c, \text{ for } (s,t) \in a\mathbb{R} \times \omega_*^{-1} \mathbb{R}^+ \quad (17a)$$

with the nonzero initial conditions of displacements and velocities

$$u_c(s,0) = \tilde{u}_c(s,0) \text{ and } D_t u_c(s,0^-) = D_t \tilde{u}_c(s,0^-), \text{ for } s \in a\mathbb{R}. \quad (17b)$$

Here D_s is the spatial partial differential operator. Within the theoretical framework of causal distributions, the governing equation in the CC setting becomes

$$\rho D_t^2 [H u_c] - \alpha D_s^2 [H u_c] = \rho \mathcal{D}_t^2 u_c, \text{ for } (s,t) \in a\mathbb{R} \times \omega_*^{-1} \mathbb{R}. \quad (18a)$$

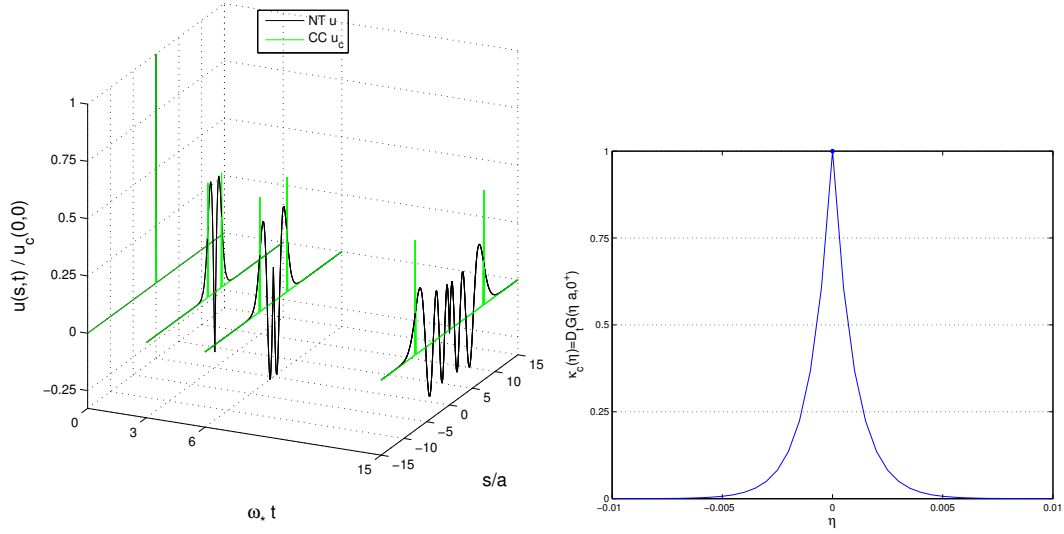


Figure 3: *TN and CC displacement fields resulting from continuum representations of the discrete initial data: $u_k(0) = \bar{u} \delta_{k,0}$ and $\dot{u}_k(0) = 0$. The displacement field $u(s, t) = D_t G(s, t) \bar{u}$ is obtained with $\kappa(\eta) = \delta(\eta)$ and yields the initial displacement $u(s, 0) = D_t G(s, 0^+) \bar{u} = \kappa_{c,0}(s/a) \bar{u}$ (in black); the CC solution $u_c(s, t) = \bar{u} [\kappa_{c,0}((s + ct)/a) + \kappa_{c,0}((s - ct)/a)]/2$ (in green) corresponds to $u_c(s, 0) \equiv u(s, 0)$.*

We also introduced the percussion forces (*i.e.* an instantaneous distribution of inertial forces)

$$\rho a \mathcal{D}_t^2 u_c(s, t) = \rho a \left\{ D_t \tilde{u}_c(s, 0^-) \delta_+(t) + \tilde{u}_c(s, 0^-) D_t \delta_+(t) \right\} \quad (18b)$$

where the correspondence between the couple of percussion kinematic fields $\tilde{u}_c(s, 0^-)$ and $D_t \tilde{u}_c(s, 0^-)$, and the couple of localized initial data $\mathbf{u}(0)$ and $D_t \mathbf{u}(0^-)$ must be specified. This can be assumed into the following classical trial form with two (possibly identical) weight functions $\kappa_{c,n}(\eta)$ to specify

$$D_t^n \tilde{u}_c(s, 0^-) = \sum_{k \in \mathbb{Z}} D_t^n u_k(0^-) \kappa_{c,n}(s/a - k), \quad \text{for } n = 0, 1. \quad (19)$$

Lately, for comparison with (3) one can also associate the following work to the foregoing model

$$\begin{aligned} \mathcal{P}_r^c(\rho \mathcal{D}_t^2 u_c, u_c, t) &\stackrel{\text{def}}{=} \int_{-\infty}^t \int_{-\infty}^{\infty} \rho \mathcal{D}_t^2 u_c(s, \check{t}) D_t u_c(s, \check{t}) ds d\check{t} \\ &= H(t) \int_{-\infty}^{\infty} \rho \left\{ D_t \tilde{u}_c(s, 0^-) D_t u_c(s, 0^+) - \tilde{u}_c(s, 0^-) D_t^2 u_c(s, 0^+) \right\} ds. \quad (20) \end{aligned}$$

Eq. (17a) (resp. (18a)) is known to be the continuous limit of the discrete model (1) (resp. (2a)). Indeed, it can be deduced by Taylor expanding Eq. (1) (resp. (2a)) while assuming the existence of a smooth continuous displacement field $u_c(ka, t) \approx u_k(t)$

for $(k, t) \in \mathbb{Z} \times \omega_*^{-1}\mathbb{R}$ and spatio-temporal variations that are sufficiently slow to be differentiable, limiting therefore the accuracy/validity of $u_c(\lambda, \omega)$ simultaneously to the longest wavelengths $|\lambda|^{-1} \gg a$ and the smallest angular frequencies $|\omega| \ll \omega_*$ where $\Phi(\lambda, \omega) \approx a\lambda^2 - \rho\omega^2$. Ideally, a successful numerical method for solving the problem (17) would provide the exact D'Alembert's traveling wave solution for $(s, t) \in a\mathbb{R} \times \omega_*^{-1}\mathbb{R}$

$$u_c(s, t) = \frac{\tilde{u}_c(s + ct, 0^-) + \tilde{u}_c(s - ct, 0^-)}{2} + \frac{1}{2c} \int_{s-ct}^{s+ct} D_t \tilde{u}_c(\hat{s}, 0^-) d\hat{s}, \quad (21)$$

which implies that $D_t^n u_c(s, 0^\pm) \equiv D_t^n \tilde{u}_c(s, 0^-)$ (with $n = 0, 1$) as long as the chain is not impacted. Note that a standard, but not necessary suitable (see Eq.(23)), assumption about the approximation trial field is the form

$$u_c(s, t) = \sum_{k \in \mathbb{Z}} u_c(ka, t) \kappa_c(s/a - k), \text{ for } (s, t) \in a\mathbb{R} \times \omega_*^{-1}\mathbb{R} \quad (22)$$

with the previous weight functions specified as $\kappa_{c,0}(\eta) = \kappa_{c,1}(\eta) = \kappa_c(\eta)$.

It turns out that the solution field (21) is equivalent for $(s, t) \in a\mathbb{R} \times \omega_*^{-1}\mathbb{R}^+$ to the following solution of the problem (18)

$$\mathbb{H}(t) u_c(s, t) \equiv \int_0^t \int_{-\infty}^{\infty} G_c(s - \hat{s}, t - \hat{t}) a^{-1} \mathfrak{D}_t^2 u_c(\hat{s}, \hat{t}) d\hat{s} d\hat{t} \quad (23a)$$

with the causal fundamental solution of (18a)

$$\text{with } G_c(s, t) \stackrel{\text{def}}{=} \omega_*^{-1} \mathbb{H}(t - |s|/c). \quad (23b)$$

This latter corresponds to the *macroscopic asymptote* of G and G_K when $\omega_* t \rightarrow \infty$ (with fixed $|s|/\omega_* a t$) or when $|s|/a \rightarrow \infty$ (with fixed $\omega_* a t/|s|$). However, contrary to G and G_K , the function G_c shows two fronts of discontinuity along $|s| = ct$, which propagate with the celerity c as illustrated on the figures 2. Similarly, *any singularity of the field u_c will propagate following this schema*. This statement can be illustrated with the approximate solution resulting from the pre-initial inertial load in (19). The expression of the solution (19) can be rewritten like

$$\mathbb{H}(t) u_c(s, t) = \sum_{p \in \mathbb{Z}} [D_t u_p(0^-) \widehat{G}_{c,1}^*(s - pa, t) + u_p(0^-) D_t \widehat{G}_{c,0}^*(s - pa, t)] \quad (24a)$$

where the acausal function

$$\widehat{G}_{c,n}^*(s, t) = \text{sign}(t) G_{c,n}^*(s, |t|), \text{ for } n = 0, 1 \quad (24b)$$

is defined the causal pseudo-Green function

$$G_{c,n}^*(s, t) \stackrel{\text{def}}{=} \int_{-\infty}^{\infty} G_c(s - \eta a, t) \kappa_{c,n}(\eta) d\eta \equiv \mathbb{H}(t) \int_0^t \frac{\kappa_{c,n}\left(\frac{s+c\hat{t}}{a}\right) + \kappa_{c,n}\left(\frac{s-c\hat{t}}{a}\right)}{2} d\hat{t}. \quad (24c)$$

It follows that the spatial regularity of the interpolating functions $\kappa_{c,n}(\eta)$ has an impact on the approximation predicted by the CC theory equation (18a) for the discrete field $\mathbf{u}(t)$ in (10). For instance, on the figure 2(b), to mimic the response of the chain impacted from rest with $\rho a \mathcal{D}_t^2 \mathbf{u}(t) = \{\rho a \bar{v} \delta_{k,0} \delta_+(t)\}_{k \in \mathbb{Z}}$ for the percussion force in (2b) a very singular and a very smooth $\kappa_{c,1}(\eta)$ were chosen to interpolate in weak and strong senses. The CC displacement field $u_c = \bar{v} G_{c,1}^*$ obtained with the infinitely smooth hat-function $\kappa_{c,1}(\eta) = \text{sinc}(\eta)$ is continuous contrary to the one $u_c = \bar{v} G_c$ obtained with the singular Dirac's function $\kappa_{c,1}(\eta) = \delta(\eta) = \frac{1}{2} D_\eta^2 |\eta|$. In fact, this yields a limited improvement that results from the nonlocal nature of the smooth inertial loading, which artificially attempts to compensate the limitations imposed to the wave propagation velocity by the classical elasticity model (18a).

While the improvement obtained with the smooth field can also be observed in the energy introduced into the mechanical system, with notably $\mathcal{P}_r^c(\rho \mathcal{D}_t^2 u_c, u_c, t) = \mathcal{P}_r(\rho \mathcal{D}_t^2 \mathbf{u}, \mathbf{u}, t)$, it is however loading and weight dependent [6]. Indeed, one can consider for instance the same Cauchy's problems with $\mathbf{u}(0) = 0$ and $D_t u_k(0^-) = \bar{v} \delta_{k,0}$ while the CC approximation is indifferently initialized with $D_t \tilde{u}_c(s, 0^-) = \bar{v} \kappa_{c,1}(s/a)$ or $\rho a \mathcal{D}_t^2 u_c(t) = \rho a D_t \tilde{u}_c(s, 0^-) \delta_+(t)$, and the more popular FEM weight function $\kappa_{c,1}(\eta) = [1 - |\eta|] \text{H}(1 - |\eta|)$. It comes then $\mathcal{P}_r^c(\rho \mathcal{D}_t^2 u_c, u_c, t) = \frac{2}{3} \mathcal{P}_r(\rho \mathcal{D}_t^2 \mathbf{u}, \mathbf{u}, t)$. Section 2.4.3 provides further comparisons and details on these dependencies.

2.4 Analogous quasi-continua

The problem of *building a continuous model that is equivalent to the granular model* includes the task to formulate a system of integro-differential equations, with respect to the two variables $(s, t) \in a\mathbb{R} \times \omega_*^{-1}\mathbb{R}$, between the *continuous field* $u(s, t)$ interpolating the discrete displacement field $\mathbf{u}(t) = \{u_k(t)\}_{k \in \mathbb{Z}}$ like

$$u(ka, t) = u_k(t), \text{ for } (k, t) \in \mathbb{Z} \times \omega_*^{-1}\mathbb{R}, \quad (25)$$

and a load density $f(s, t)$ that is linked in some sense to those acting onto the discrete structure, $\mathbf{f}(t) = \{f_k(t)\}_{k \in \mathbb{Z}}$ [3]-[6]. The reasoning provided in [4]-[6], and repeated hereafter for self-containedness, still holds whether the considered applied load \mathbf{f} are external or generated as the percussion force $\rho a \mathcal{D}_t^2 \mathbf{u}$ in (2b) by initial kinematic conditions.

2.4.1 Additional criteria of interpolation

From a spectral viewpoint, a crucial step is the substitution of the (7a) in the space $a^{-1}\mathbb{C} \times \omega_*\mathbb{C}$ of spectral variables (λ, ω) by an equation of interpolation

$$\Phi^\dagger(\lambda, \omega) u^\dagger(\lambda, \omega) = f^\dagger(\lambda, \omega) \quad (26)$$

which itself allows to replace the DFT (5) and its inverse (6b) the integral Fourier transform \mathbf{FT} and its inverse

$$y(s) \rightarrow y^\dagger(\lambda) = \int_{-\infty}^{\infty} y(s) e^{-i\lambda s} d\lambda; \quad y^\dagger(\lambda) \rightarrow y(s) = \frac{1}{2\pi} \int_{-\infty}^{\infty} y^\dagger(\lambda) e^{i\lambda s} d\lambda. \quad (27)$$

The interpolation fields $u(s, t)$ and $f(s, t)$ are then inferred from $u^\dagger(\lambda, \omega)$ and $f^\dagger(\lambda, \omega)$ via (4), (6a) and (27).

The constraint (25) still left however a large choice of the functions $\Phi^\dagger(\lambda, \omega)$ and $f^\dagger(\lambda, \omega)$ whose the analogs $\Phi(\lambda, \omega)$ in (7b) and $f(\lambda, \omega) = \sum_{k \in \mathbb{Z}} f_k(\omega) e^{-i\lambda ka}$ are notably $2\pi a^{-1}$ -periodic in $\lambda \in a^{-1}\mathbb{C}$. To restrict the choice, an equivalence is additionally imposed for the resultants of the either external or initial inertial acting loads

$$\int_{-\infty}^{\infty} f(s, t) ds \equiv a \sum_{k \in \mathbb{Z}} f_k(t), \text{ for } t \in \omega_*^{-1}\mathbb{R} \quad (28a)$$

and furthermore an equivalence between the load works is also wished

$$\mathcal{P}_r^c(\rho \mathcal{D}_t^2 u(t), u, t) \equiv \mathcal{P}_r(\rho \mathcal{D}_t^2 \mathbf{u}(t), \mathbf{u}, t). \quad (28b)$$

In particular the continuum load work can be expressed like (20).

Within the framework of distribution theory, there exist then at least two natural choices for the loading fields $f(s, t)$ that satisfy (28a) while keeping the interpolation ansatz $f(s, t) \equiv \sum_{k \in \mathbb{Z}} f_k(t) \kappa(s/a - k)$ for $(s, t) \in a\mathbb{R} \times \omega_*^{-1}\mathbb{R}$:

one is the *singular* Dirac's comb distribution where $\kappa(\eta) = \delta(\eta) \stackrel{\text{def}}{=} D_\eta^2 \frac{|\eta|}{2}$ for $\eta \in \mathbb{R}$

so that $\int_{-\beta a}^{\beta a} f(ka + s, t) ds \equiv a f_k(t), \forall \beta \in]0, 1[;$

the second one is the *regular* distribution where $\kappa(\eta) = \text{sinc}(\eta)$ (if the resulting *cardinal series converges* in the sub-space of continuous functions with λ -support spectral in \mathbb{K}) so that $f(ka, t) = f_k(t)$.

Since the acting load distribution $\mathbf{f}(t)$ can be arbitrary, the desired interpolation property (25) can be reformulated as a restriction on the spectral functions describing the material elasticity and inertia $\Phi^\dagger(\lambda, \omega)$ alone. Thus, in the singular load interpolation case it is convenient to take as a *measure of concordance*

$$\int_{-i\omega_b - \infty}^{-i\omega_b + \infty} \int_{-\infty}^{\infty} \frac{e^{i(\lambda ka + \omega t)}}{\Phi^\dagger(\lambda, \omega)} d\lambda d\omega \equiv \int_{-i\omega_b - \infty}^{-i\omega_b + \infty} \int_{-\pi/a}^{\pi/a} \frac{e^{i(\lambda ka + \omega t)}}{\Phi(\lambda, \omega)} d\lambda d\omega \quad (29)$$

and in the regular load interpolation case

$$\int_{-\pi/a}^{\pi/a} \int_{-i\omega_b - \infty}^{-i\omega_b + \infty} \frac{e^{i(\lambda ka + \omega t)}}{\Phi^\dagger(\lambda, \omega)} d\omega d\lambda \equiv \int_{-\pi/a}^{\pi/a} \int_{-i\omega_b - \infty}^{-i\omega_b + \infty} \frac{e^{i(\lambda ka + \omega t)}}{\Phi(\lambda, \omega)} d\omega d\lambda. \quad (30)$$

Those formulations take into account the order of application of the transforms (4) and (5) upon Eq.(2a) and that allow to identify the right hand side double integrals in (29) and (30) with $4\pi^2 G(ka, t)$ and $4\pi^2 G_K(ka, t)$, respectively.

2.4.2 Strong spectral approaches

For the smooth loading choice (30), two types of spectral functions of elasticity and inertia $\Phi^\dagger(\lambda, \omega)$ satisfying (30) are frequently proposed (e.g. [25, 26, 3, 27]). A first

one corresponds to

$$\Phi^\dagger(\lambda, \omega) \equiv \Phi(\lambda, \omega), \quad (31)$$

and the second one to

$$\Phi^\dagger(\lambda, \omega) \equiv 1_{\mathbb{B}_0}(\lambda) \Phi(\lambda, \omega), \quad \text{with } \mathbb{B}_0 \stackrel{\text{def}}{=} \{\lambda \in a^{-1}\mathbb{C}; |\Re(\lambda)a| \leq \pi\} \quad (32)$$

while $1_{\mathbb{B}_0}$ denoting the characteristic function of the domain \mathbb{B}_0 . The quasicontinuum spectral model (31) has been adopted by Eringen [26], while the model (32) is the one chosen by Kunin [3]. In both cases, to be exact and to not produce singularities (see [6]), the functions $u(s, t)$, $\rho a \mathcal{D}_t^2 u(s, t)$ and $f(s, t)$ must be limited to Whittaker-Kotel'nikov-Shannon's (WKS) functions of interpolation [23, 24], which assumes the spectra $u^\dagger(\lambda, \cdot)$, $\rho a \mathcal{D}_t^2 u^\dagger(\lambda, \cdot)$ and $f^\dagger(\lambda, \cdot)$ supported by \mathbb{K} for $\lambda \in a^{-1}\mathbb{R}$.

The elastodynamic equations characterized by (26), (31) and (32) read either as follow for $(s, t) \in a\mathbb{R} \times \omega_*^{-1}\mathbb{R}^+$

$$\rho D_t^2 u(s, t) = \int_{-\infty}^{\infty} \mathcal{K}_s\left(\frac{s-\check{s}}{a}\right) D_{\check{s}}^2 u(\check{s}, t) d\check{s} \quad (33a)$$

$$= - \int_{-\infty}^{\infty} \mathcal{L}_s\left(\frac{s-\check{s}}{a}\right) u(\check{s}, t) d\check{s} \quad (33b)$$

with the initial kinematic conditions $D_t^n u(s, t) = \rho a \sum_{k \in \mathbb{Z}} D_t^n u_k(t) \text{sinc}(s/a - k)$ (for $n = 0, 1$). It can also be expressed as follows for $(s, t) \in a\mathbb{R} \times \omega_*^{-1}\mathbb{R}$

$$\rho \mathcal{D}_t^2 u(s, t) = \rho D_t^2 [\text{H}(t) u(s, t)] - \int_{-\infty}^{\infty} \mathcal{K}_s\left(\frac{s-\check{s}}{a}\right) \text{H}(t) D_{\check{s}}^2 u(\check{s}, t) d\check{s} \quad (34a)$$

$$= \rho D_t^2 [\text{H}(t) u(s, t)] + \int_{-\infty}^{\infty} \mathcal{L}_s\left(\frac{s-\check{s}}{a}\right) \text{H}(t) u(\check{s}, t) d\check{s} \quad (34b)$$

with the percussion load

$$\rho a \mathcal{D}_t^2 u(s, t) = \rho a \sum_{k \in \mathbb{Z}} \mathcal{D}_t^2 u_k(t) \text{sinc}(s/a - k). \quad (35)$$

Those equations involve the following functions of elasticity for $\eta \in \mathbb{R}$

$$\mathcal{K}_s(\eta) \stackrel{\text{def}}{=} \frac{1}{2\pi} \int_{-\infty}^{\infty} \frac{\Phi^\dagger(\lambda, 0)}{\lambda^2} e^{i\eta\lambda a} d\lambda \quad \text{and} \quad \mathcal{L}_s(\eta) \stackrel{\text{def}}{=} \frac{1}{2\pi} \int_{-\infty}^{\infty} \Phi^\dagger(\lambda, 0) e^{i\lambda\eta a} d\lambda.$$

The kernel model (31) leads then to the following functions of elasticity

$$\mathcal{K}_s(\eta) = \frac{\alpha}{a} \frac{|\eta + 1| + |\eta - 1| - 2|\eta|}{2} \equiv \frac{\alpha}{a} \text{H}(1 - |\eta|) [1 - |\eta|] \quad (36a)$$

$$\mathcal{L}_s(\eta) = \frac{\alpha}{a^3} [2\delta(\eta) - \delta(\eta + 1) - \delta(\eta - 1)]. \quad (36b)$$

In fact, the integro-differential equation (34) endowed with the kernel (36b) can be expressed more simply like

$$\rho \mathcal{D}_t^2 u(s, t) = \rho D_t^2 [\text{H}(t) u(s, t)] - \alpha \text{H}(t) \frac{u(s + a, t) + u(s - a, t) - 2u(s, t)}{a^2}.$$

Similarly to the models developed in [31, 32], the absence of spatial differentiation $D_s u(s, t)$ in that equation entails that its solutions $u(s, t)$ are continuous only if the initial (and load) conditions are sufficiently smooth (see [6]); consequently, this excludes the Dirac's singular loading field and therefore the localized impacts.

The kernel model (32) leads to the following functions of elasticity for $\eta \in \mathbb{R}$

$$\mathcal{K}_s(\eta) = \frac{\alpha}{a} \left[(\eta + 1) \tilde{\text{Si}}(\eta + 1) + (\eta - 1) \tilde{\text{Si}}(\eta - 1) - 2\eta \tilde{\text{Si}}(\eta) - \frac{4 \cos(\eta \pi)}{\pi^2} \right] \quad (37a)$$

$$\mathcal{L}_s(\eta) = \frac{4\alpha}{a^3} \frac{\eta^2 - 1/2}{\eta^2 - 1} \text{sinc}(\eta) \quad (37b)$$

with $\tilde{\text{Si}}(\eta) \stackrel{\text{def}}{=} \int_0^\eta \text{sinc}(\check{\eta}) d\check{\eta}$. The use of the integro-differential equation (34) endowed with (37) requires infinite domains of integration, and so is not adequate for bounded domains. Other drawbacks related to the support of the loads must also be mentioned (see [6]).

Despite of these drawbacks, for the WKS smooth interpolation fields, the dynamical continuum models described by Eqs. (33) also allow to recover however the exact kinematic and energy state related to the discrete model described by Eq. (1) (see [6]). Within the WKS smooth interpolation field space, the formal solution of the dynamic equation (34) is as follows for both kernel choices (31) and (32)

$$\text{H}(t) u(s, t) \equiv \sum_{p \in \mathbb{Z}} \int_0^t G_K(s - pa, t - \hat{t}) a^{-1} \mathfrak{D}_t^2 u_p(\hat{t}) d\hat{t}. \quad (38)$$

For $(s, t) \in a\mathbb{R} \times \omega_*^{-1}\mathbb{R}^+$, this is equivalent to the following field that solves (33)

$$u(s, t) = \sum_{p \in \mathbb{Z}} \left[D_t \hat{G}_K(s - pa, t) u_p(0) + \hat{G}_K(s - pa, t) \dot{u}_p(0^+) \right] \quad (39)$$

defined with the antisymmetric extension of the causal ‘‘pseudo-fundamental’’ solution G_K in (14).

2.4.3 The weak spectral approach

The formulation (29) is based on a weak multipolar approximation (WMPA) developed in [4, 6] inspired by the Mittag-Leffler's rational expansion series of the meromorphic spectral function $[\Phi(\lambda, \omega)]^{-1}$ on $a^{-1}\mathbb{C} \times \omega_*\mathbb{C} \setminus \mathcal{C}$. The truncating approximation according to Eq. (29) yields the following weak multipoint Padé's approximation function [6]

$$\Phi^\dagger(\lambda, \omega) = \alpha [\lambda^2 - \lambda_o^2] \text{sinc}(\lambda_o a / \pi) \equiv \rho a [G^\dagger(\lambda, \omega)]^{-1}. \quad (40)$$

By inverse transforms of the spectral equation (26) with this kernel, the equation of dynamic motion can be expressed finally as follows for $(s, t) \in a\mathbb{R} \times \omega_*^{-1}\mathbb{R}$

$$\rho \mathfrak{D}_t^2 u(s, t) = \left[1 + \frac{1}{\omega_*^2} D_t^2 \right] \int_0^t [D_t^3 \Upsilon_1(\hat{t}) u(s, t - \hat{t}) - D_t \Upsilon_2(\hat{t}) D_s^2 u(s, t - \hat{t})] d\hat{t} \quad (41a)$$

where the following initial inertial load of percussion is used to (re-)generate initial kinematic states

$$\rho a \mathfrak{D}_t^2 u(s, t) = \rho a \sum_{k \in \mathbb{Z}} \mathfrak{D}_t^2 u_k(t) \delta(s/a - k). \quad (41b)$$

The integrals in Eq. (41a) use the following stiffness and mass distributions

$$\Upsilon_1(t) \equiv \tilde{\Upsilon}_1(\omega_* t) \stackrel{\text{def}}{=} \rho H(t) \left\{ 1 - \int_{\omega_*}^{\infty} \frac{\omega_* \cos(\omega_r t)}{\omega_r^2 \sqrt{\frac{\omega_r^2}{\omega_*^2} - 1}} d\omega_r \right\}, \quad (42a)$$

$$\Upsilon_2(t) \equiv \tilde{\Upsilon}_2(\omega_* t) \stackrel{\text{def}}{=} \alpha H(t) \left\{ 1 - \int_{\omega_*}^{\infty} \frac{4 \cos(\omega_r t) d\omega_r}{\omega_* \left[\frac{a^2}{\ell_+^2} + \pi^2 \right] \sqrt{\frac{\omega_r^2}{\omega_*^2} - 1}} \right\}. \quad (42b)$$

They satisfy $\Upsilon_1(0) = \Upsilon_2(0) = D_t \Upsilon_1(0) = D_t^2 \Upsilon_1(0) = 0$ and tend to $\tilde{\Upsilon}_1(+\infty) \equiv \rho$ and $\tilde{\Upsilon}_2(+\infty) \equiv \alpha$. The classical wave equation (18a) can be inferred from (41a) by passing to the limit with $(a, \omega_*^{-1}) \rightarrow (0, 0)$ while keeping $\omega_* a = 2c$ finite. The temporally-nonlocal (TN) continuum model (41a) possesses a complex internal inertia and elasticity reminiscing a modeling of *continuum mechanics enhanced with hereditary or memory properties* proposed in [33] for composite and heterogeneous materials. However as for the discrete model, this new continuum remains spatially local (which underlies that boundary conditions will remains too) and does require only the classical initial conditions. Hence, an analytic comparison between the predictions of this dynamic model and those of a finite chain for various loading conditions are possible as shown in a future communication. Lately, contrarily to those of the subsection 2.4.2, the TN model (41a) admits singular loading. In particular for the singular inertial load (41b), the final expression of the formal solution of the TN dynamic equation (41a)

$$H(t) u(s, t) \equiv \int_0^t \int_{-\infty}^{\infty} G(s - \hat{s}, t - \hat{t}) a^{-1} \mathfrak{D}_t^2 u(\hat{s}, \hat{t}) d\hat{s} d\hat{t} \quad (43)$$

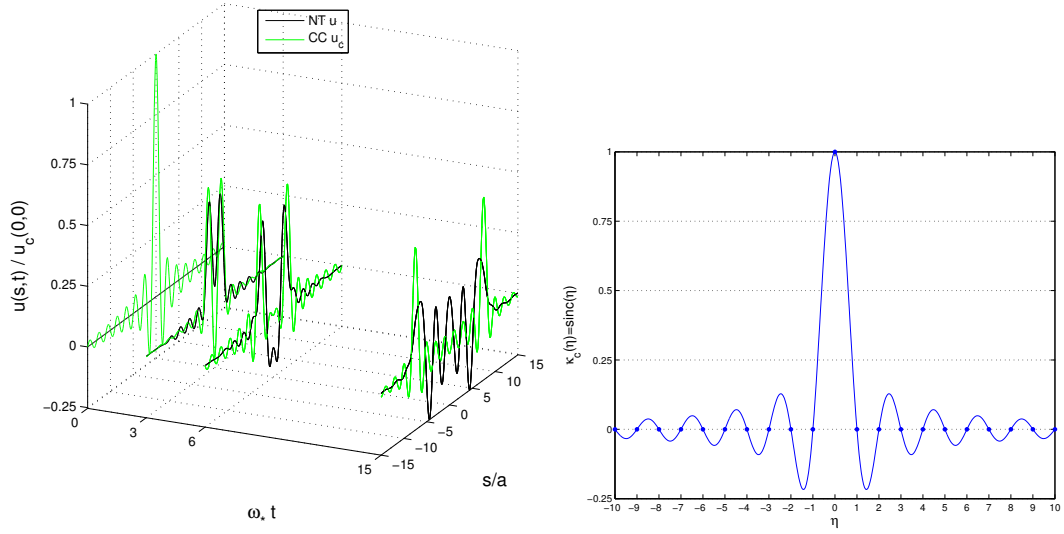
can be viewed as a restriction onto $(s, t) \in a\mathbb{R} \times \omega_*^{-1}\mathbb{R}^+$ of the field

$$u(s, t) = \sum_{p \in \mathbb{Z}} \left[D_t \hat{G}(s - pa, t) u_p(0) + \hat{G}(s - pa, t) \dot{u}_p(0^-) \right] \quad (44)$$

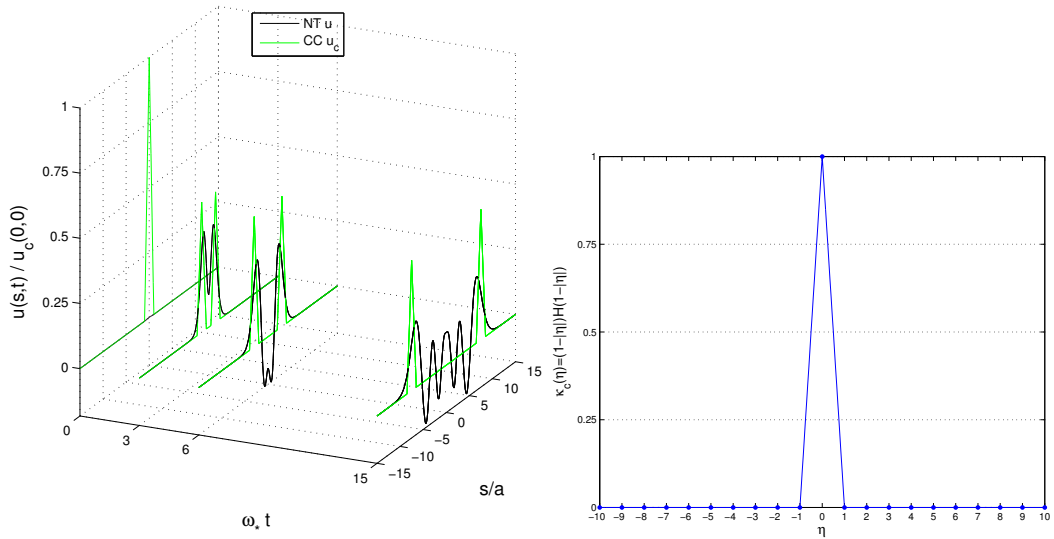
defined with the antisymmetric extension of the causal fundamental solution with $G(s, t)$ in (13). Albeit the continuum inertial load representation of the initial conditions is singular, one can check however that the solution (44) is a regular continuous interpolation of the original discrete solution \mathbf{u} in (10), since for $n = 0, 1$

$$D_t^n u(s, 0^-) = \sum_{p \in \mathbb{Z}} D_t \hat{G}(s - pa, 0^-) D_t^n u_p(0^-) \text{ and } D_t^n \hat{G}(s - pa, 0^\pm) \equiv D_t^n G(s - pa, 0^\pm).$$

The singular load (41b) is relevant to accurately recover the free motion field and



(a) $u = D_t G^* \bar{u}$ for $\kappa(\eta) = \kappa_{c,0}(\eta) = \text{sinc}(\eta)$ and $u_c(s, 0) \equiv \kappa_{c,0}(s/a) \bar{u}$



(b) $u = D_t G^* \bar{u}$ for $\kappa(\eta) = \kappa_{c,0}(\eta) = (1 - |\eta|)H(1 - |\eta|)$ and $u_c(s, 0) \equiv \kappa_{c,0}(s/a) \bar{u}$

Figure 4: TN and CC displacement fields resulting from smooth continuum representations of the discrete initial data: $u_k(0) = \bar{u} \delta_{k,0}$ and $\dot{u}_k(0) = 0$.

the corresponding discrete energy state from this TN model prediction [6]. Although, relatively good approximations at sufficiently large times can be qualitatively obtained with other weight functions not fulfilling the interpolation criteria (28), due to the non-trivial inertia and elasticity of the TN model. Indeed, if one replaces $\delta(\eta)$ in (41b) by a regular interpolating weight function $\kappa(\eta)$, then the solution (43) reads like

$$H(t) u(s, t) = \sum_{p \in \mathbb{Z}} [D_t u_p(0^-) G^*(s - pa, t) + u_p(0^-) D_t G^*(s - pa, t)] \quad (45a)$$

with the following pseudo-Green function

$$G^*(s, t) \stackrel{\text{def}}{=} \int_{-\infty}^{\infty} G(s - \eta a, t) \kappa(\eta) d\eta. \quad (45b)$$

For illustration, for the discrete initial data $\mathbf{u}(0) = \{\bar{u} \delta_{k,0}\}_{k \in \mathbb{Z}}$ and $\dot{\mathbf{u}}(0) = \mathbf{0}$, the solution (43) that simply reads like $u(s, t) = G(s, t) \bar{u}$ (see Fig. 3) can be compared to the continuum solution (45) obtained with $\kappa(\eta) = \kappa_{c,0}(\eta) = \text{sinc}(\eta)$ (see Fig. 4(a)) and $\kappa(\eta) = \kappa_{c,0}(\eta) = [1 - |\eta|]H(1 - |\eta|)$ (see Fig. 4(b)). The resulting displacement field $u(s, t) = D_t G^*(s, t) \bar{u}$ (in black) may be interpreted as corresponding to a non-interpolating initial displacement field $u(s, 0) = D_t G^*(s, 0^+) \bar{u}$. Comparisons with the related CC approximations (in green) corresponding to $\tilde{u}_c(s, 0) = u_c(s, 0) = \kappa_{c,0}(s/a) \bar{u}$ or equivalently to the percussion load (18b) $\rho a \mathcal{D}_t^2 u_c(s, t) = \rho a \mathcal{D}_t^2 u_0 \kappa_{c,0}$ are also provided. The expressions (21), (23a), and (24) of those approximations can also be simply read as $u_c(s, t) = \bar{u}[\kappa_{c,0}((s + ct)/a) + \kappa_{c,0}((s - ct)/a)]/2$. As observed, the behaviours of the regular- $\kappa(\eta)$ approximations in (45) converge towards the interpolation (44) where therefore $\kappa(\eta) = \delta(\eta)$. This is not the case with the CC model owing to its dispersive-less nature. In fact, comparing Fig. 3 and Figs. 4 shows that the agreement with the discrete theory is rather poor. The relevance of the choice of kernel $\kappa_{c,0}$ in the CC theory can also be mentioned regarding the energy equivalence for the considered initial problems [6]. Indeed, for instance the smooth weight function $\kappa_{c,0} = \text{sinc}(\eta)$ provides $\mathcal{P}_r^c(\rho \mathcal{D}_t^2 u_c, u_c, t) = \frac{\pi^2}{6} \mathcal{P}_r(\rho \mathcal{D}_t^2 \mathbf{u}, \mathbf{u}, t)$, while $\kappa_{c,0} = [1 - |\eta|]H(1 - |\eta|)$ provides the energy equivalence $\mathcal{P}_r^c(\rho \mathcal{D}_t^2 u_c, u_c, t) = \mathcal{P}_r(\rho \mathcal{D}_t^2 \mathbf{u}, \mathbf{u}, t)$.

3 Conclusion

This paper highlighted some key points of the derivation of enhanced quasicontinuum models that can be closely based on the dispersive vibrational properties of lattices and periodic material systems. These new insights may help in the numerical simulations coupling of continuum and discrete/molecular modeling, which is in general a non-trivial task. In the current practice, the continuum model often relies on the CC mechanics, mistakenly. The use of the CC model entails, for instance, that the high frequencies coming from the discrete media cannot avoid to be reflected by fixed or moving interfaces (like fronts of discontinuity or model separation) instead of being transmitted [34, 17, 18, 21]. This pinpoints the need for enhancing continuum mechanics to catch the micro-structural effects due to the discreteness of the material properties in lattices and other periodic systems and that are particularly important in the high-frequency regime.

The construction of enhanced continuum mechanics involves to adopt pertinent inertial and stiffness terms and characteristic micro-structural length and time scales. This paper has shown which can be taken into account for building a quasi-continuum model that is equivalent to a simple, periodic, linear elastic monoatomic chain. In particular, it has been shown that a memory-dependent quasi-continuum model is able to correctly capture the non-trivial physical phenomena of wave dispersion in

the micro-structured spring-mass lattice, which are overlooked by the CC theory and its finite-element discretization. Comparisons between this TN model and some of the enhanced continuum models proposed in the literature up to this date were proposed in [6]. Unlike the other ones, the TN model assumes some modifications of the classical elasto-dynamic Newton's law model that do not increase the number of initial and boundary conditions of the mechanical evolution problem. Other similar constructions that are under investigation for other non-simple lattices and atom motions will be presented elsewhere.

References

- [1] Fish J., "Bridging the scales in nano engineering and science", *J. Nanoparticle Research*, 8, 577-594, 2006.
- [2] L. Brillouin, M. Parodi, "Propagation des ondes dans les milieux périodiques", Masson, Dunod, Paris, 1956.
- [3] I. Kunin. "Elastic media with microstructure, v.I (One dimensional models)", Berlin: Springer, 1982.
- [4] M. Charlotte, L. Truskinovsky, "Towards multi-scale continuum elasticity theory", *Cont. Mech. Thermodyn.*, 20, pages 133-161, 2008.
- [5] M. Charlotte, L. Truskinovsky, "Modélisations quasi-continues du comportement dynamique d'un réseau atomique de simple micro-structure", 10eme Colloque National en Calcul des Structures.
- [6] M. Charlotte, L. Truskinovsky, "Lattice dynamics from a continuum viewpoint", *J. Mechanics and Physics of Solids*, PII : S0022-5096(12)00058-0, DOI : 10.1016/j.jmps.2012.03.004, 2012.
- [7] A.A. Maradudin, E.W. Montroll, G.H. Weiss, I.P. Ipatova, "Theory of lattice dynamics in the harmonic approximation", Academic Press, New-York, 1971.
- [8] M. Charlotte, L. Truskinovsky, "Linear chain with a hyper-pre-stress", *J. Mech. Phys. Solids*, 50, pages 217-251, 2002.
- [9] A. Metrikine. "On causality of the gradient elasticity models", *J. Sound and Vibration*, 297, pages 727-742, 2006.
- [10] H. Askes, A.V. Metrikine, A.V. Pichugin, T. Bennett, "Four simplified gradient elasticity models for the simulation of dispersive wave propagation", *Philosophical Magazine*, vol 88(28-29), pages 3415-3443, 2008.
- [11] J.D. Kaplunov, A.V. Pichugin, "On rational boundary conditions for higher-order long-wave models", *IUTAM Symposium on Scaling in Solid Mechanics*, IUTAM Bookseries, Vol 10, pages 81-90, 2009.
- [12] A. Metrikine, H. Askes. "One-dimensional dynamically consistent gradient elasticity models derived from a discrete microstructure, Part1: generic formulation". *European J. Mech. A/ Solids*, 21, pages 555-572, 2002.
- [13] A. Metrikine, H. Askes, "One-dimensional dynamically consistent gradient elasticity models derived from a discrete microstructure, Part2: static and dynamic response", *European J. Mech. A/ Solids*, 21, pages 573-588, 2002.

- [14] P. Rosenau, “Hamiltonian dynamics of dense chains and lattices: or how to correct the continuum”, *Phys. Lett. A*, 311, pages 39-52, 2003.
- [15] M. Ortiz, R. Phillips, E.B. Tadmor, “Quasicontinuum analysis of defects in solids”, *Phil. Mag. A*, vol 73, pages 1529-1563, 1996.
- [16] V. B. Shenoy, R. Miller, E.B. Tadmor, D. Rodney, R. Phillips, M. Ortiz. “An adaptive methodology for atomic scale mechanics: The quasicontinuum method”, *J. Mech. Phys. Sol.*, 47, pages 611-642, 1999.
- [17] H.S. Park, W.K. Liu. “An introduction and tutorial on multi-scale analysis in solids”, *Comput. Meth. Appl. Mech. Engrg.*, 193, pages 1733-1772, 2004.
- [18] Park H.S., Karpov E.G., Liu W.K., Klein P.A., “The bridging scale for two-dimensional atomistic/continuum coupling”, *Philosophical Magazine*, Taylor & Francis, Vol. 85, No. 1, 1, pages 79-113, 2005.
- [19] R.E. Miller, E.B. Tadmor, “The quasi-continuum method:overview, applications and current directions”, *J. Computer-Aided Materials Design*, 9, pages 203-239, 2002.
- [20] R. Miller, E.B. Tadmor, “A unified framework and performance benchmark of fourteen multiscale atomistic/continuum coupling methods”, *Modelling Simul. Mater. Sci. Eng.*, vol 17, n5, 2009.
- [21] S. Tang, T.Y. Hou, W.K. Liu. “A mathematical framework of the bridging scale method”, *Int. J. Numer. Meth. Engng.*, 65, pages 1688-1713, 2006.
- [22] M. Abramowitz, I. A. Stegun, “Handbook of Mathematical Functions with Formulas, Graphs, and Mathematical Tables”, New York: Dover Publications, ISBN 978-0-486-61272-0, eds. 1972.
- [23] R. J. II Marks. “Introduction to Shannon Sampling and Interpolation Theory”, Springer-Verlag, New York, 1991.
- [24] J.R. Higgins, “Sampling Theory in Fourier and Signal Analysis. Foundations”, Clarendo Press, Oxford, 1996.
- [25] A.C. Eringen, “Linear theory of nonlocal elasticity and dispersion of plane waves”, *Int. J. Eng. Sci.*, 10, pages 425-435, 1972.
- [26] A.C. Eringen, “Nonlocal field theories”, In *Continuum Physics* (Edited by A.C. Eringen), Academic press, New York, 4, pages 205-267, 1976.
- [27] D. Rogula, “Introduction to nonlocal theory of material media in: Nonlocal theory of elastic media”, *CISM Courses*, Springer, Berlin, 268, 123-222, 1982.
- [28] Schwartz L., “Théorie des distributions”, Hermann, Paris, 1966.
- [29] Schwartz L., “Méthodes mathématiques pour les sciences physiques”, Hermann, Paris, 1983.
- [30] K.B. Wolf, “Integral transforms in science and engineering”, Plenum Press, New-York, 1979.
- [31] S.A. Silling. “Reformulation of elasticity theory for discontinuities and long-range forces”, *J. Mech. Phys. Solids*, 48, pages 175-209, 2000.
- [32] S.A. Silling. *Peridynamic Theory of Solid Mechanics*, *Advanced in Applied Mech.*, vol. 44, pages 73-168, 2010.
- [33] Milton G.W., Willis J.R., “On modifications of Newton’s second law and linear continuum elastodynamics”, *Proc. R. Soc. A*, 463, 855-880, 2007

- [34] S.A. Adelman, J.D. Doll, "Generalized Langevin equation approach for atom/solid-surface scattering: General formulation for classical scattering off harmonic solids", *J. Chem. Phys.*, 64(4), pages 2375-2388, 1976.